A CONCEPT FOR ADAPTIVE MONO-PLOTTING
USING IMAGES AND LASERSCANNER DATA

C. Ressl[a], A. Haring[a], Ch. Briese[a], F. Rottensteiner[b]

[a] Christian Doppler Laboratory "Spatial Data from Laser Scanning and Remote Sensing", TU Vienna, {car,ah,cb}@ipf.tuwien.ac.at
[b] Institute of Photogrammetry and Remote Sensing, TU Vienna, fr@ipf.tuwien.ac.at

KEY WORDS: Photogrammetry, LIDAR, Surface, Reconstruction, Semi-automation, Extraction, Fusion, Combination

ABSTRACT:

The combination of photogrammetry (with its high geometric and radiometric resolution) and terrestrial laser scanning (allowing direct 3D measurement) is a very promising technique for object reconstruction, and has been applied for some time now, e.g. in the system Riegl LMS Z-420i. Nevertheless, the results presented from the combined laser-image-data very often are only coloured point clouds or textured meshes. Both object representations usually have erroneous representations of edges and corners (due to the characteristics of the laser measurement) and furthermore the amount of data to be handled in these "models" is typically enormous. In contrast to these object representations a surface model using a polyhedral compound would use only the relevant object points. However, the extraction of these *modelling points* from laser-image-data has not yet been fully automated. Especially the necessary generalization can only be accomplished by a human operator. Therefore, our aim is to support the operator in his work by speeding up the measurement of these modelling points. For this aim, this article presents a simple mono-plotting method that allows the human operator to identify each modelling point (on corners and edges) in the high-resolution images by a single mouse click. Subsequently, for this selected image ray, the missing distance is automatically determined from the associated laser data. This procedure starts by extracting the laser points in a cone around the image ray. Then these extracted points are tested for locally smooth surface patches (e.g. planar regions). Finally, the image ray is intersected with the foremost or hindmost of the extracted plane surface patches. Within this procedure the influence of erroneous laser measurements close to edges and corners can be avoided and furthermore, the distance from the scanner centre to the intersection point is determined with a better accuracy than the single laser point.

1. MOTIVATION

3D objects need to be represented for many applications, e.g. for visualization purposes, or for object analyses in order to derive certain object properties. The representation of a 3D object can be any of the following types (Rottensteiner 2001):

- *point cloud:* the object is just described by the vertices
- *wire frame model:* the object is described by vertices and edges
- *surface model:* the object is described by vertices, edges and faces
- *volumetric model:* the object is described by vertices, edges, faces and volumes, e.g. a set of volumetric primitives.

The representation using a point cloud may only serve for visualization purposes, with the visualization quality depending on the point density. However, mathematical analyses such as computing the volume or the area of an object are very difficult to accomplish when using only a point cloud representation. Such analyses require a model representation.

Of the three model representations, the surface model is the most applicable both for visualization and for mathematical analyses. Compared with wire frame models, surface models add the important definitions of faces, and compared with the volumetric models, surface models allow the representation of irregularly shaped objects in a much easier way.

Independent of the sensor (digital camera or terrestrial laser scanner) used for surveying of an object, the whole modelling process can be divided into three phases: data *acquisition*, data *orientation*, and the actual *modelling*.

In the context of this work we consider terrestrial objects, whose surface can be very well approximated by a *polyhedral compound*, e.g. facades of buildings, like the oriel window shown in fig. 1. Because of the large quantity of different object types that may appear in terrestrial scenes and the associated level of detail, it is very difficult to model such objects automatically – at least in a practical way. Usually the available data, e.g. images, provide a much higher resolution than required for the reconstruction of the object. The necessary generalization can only be accomplished by a human operator. Therefore, in the context of this work we consider the selection of the relevant object information for an adequate representation to be performed manually. A human operator digitizes the important object points, which make up the vertices of the surface model to be generated. These modelling points are placed at distinct positions of the object – usually on edges and at corners of the object.

Terrestrial photogrammetry always has been a prime source for deriving surface models of 3D objects. This is due to the capability of very fast data acquisition and high image resolution both in a geo-metrical and a radio-metrical sense. The orientation and modelling phases, however, are much more time consuming. This is mainly due to the fact that images only record directions to the object points, thus the 3D reconstruction has to be done indirectly by spatial intersection using at least two images taken from different view points. In addition, terrestrial images are usually not taken in a regular pattern, so that the orientation of such images can only be automated in a limited way (at least up to now no commercial software

package provides a fully automated orientation procedure for general image arrangements), or special time consuming actions are required to take place on site (such as sticking markers on the object resp. providing many control points). Due to the indirect nature of photogrammetric object reconstruction, the modelling phase is slowed down as the human operator has to identify the modelling points in at least two images – very often only monoscopically. Overall, for the reasons mentioned above surface reconstruction from images is generally a rather time-consuming process.
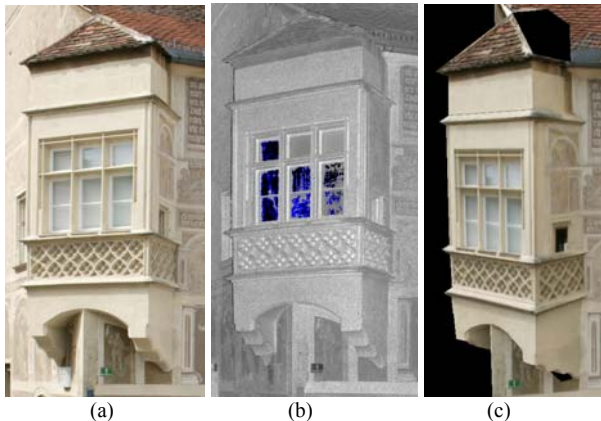

| (a) | (b) | (c) |

Fig. 1. a) Section of the original photo (pixel spacing 6mm), b) Section of the intensity image of the laser scanner (pixel spacing 1cm), c) Reconstructed object covered with the original texture from a). Data acquired with Riegl LMS Z420i and mounted Canon digital camera EOS 1Ds with a 20mm lens; mean object distance 14.5m.

With the advent of terrestrial laser scanning, it seemed that the procedure of deriving surface models would be sped up and terrestrial photogrammetry would become less important. This expectation was due to the following features of laser scanning, which outperform photogrammetry: (i) It is an active and direct 3D measuring principle, thus a 'single' measurement is sufficient to derive the 3D coordinates of an object point. (ii) The orientation of several overlapping laser scans can be automated to a very high degree. These tremendous advantages also compensate a slightly longer acquisition time on site (compared to taking images). However, it also became evident that laser scanning has its drawbacks: (i) Distances measured close to edges and corners are very unreliable; e.g. (Böhler et al. 2003). (ii) Compared with digital photogrammetry the laser's object resolution is generally a little worse from a geometric viewpoint and dramatically worse from a radiometric viewpoint; cf. fig. 1b and 1a. Due to these drawbacks, modelling from terrestrial laser scanner data is not yet completely satisfactory: The human operator has problems in identifying the "important" points only from the laser intensity data (due to the bad geometric and radiometric resolution), and furthermore these important points are on edges and corners of the object – spots where the laser might return erroneous distances. Consequently, point clouds rather than surface models are presented usually as the result of terrestrial laser scanning.

It also became clear that a combination of both photogrammetry (with its high geometric and radiometric resolution) and terrestrial laser scanning (allowing highly automated direct 3D measurement) would be promising. Additionally by mounting a digital camera directly on top of the laserscanner, e.g. the system Riegl LMS Z-420i (Riegl 2006) shown in fig. 2a, the orientation of the whole system can be determined very fast.

Nevertheless, the results presented from the combined laser-image-data very often are still only coloured point clouds or textured meshes – both with erroneous representations of edges and corners. Although meshes are specific surface models, they are not the best choice for representing objects with polyhedral compounds from a storage point of view. Further, they usually have no object interpretation and generalisation.

In order to speed up manual modelling of objects by polyhedral compounds based on oriented image-laser-data, in this article we present a simple method that allows the human operator to identify each modelling point (at corners or edges) in the high-resolution images by a single mouse click. With this selected image ray, the missing distance is determined from the associated laser-data automatically. This procedure starts by extracting the laser points in a certain cone around the image ray. The extracted points are tested for the occurrence of planes. Then, the intersection points between the image ray and the detected planes are calculated yielding candidates for the required object point. Candidates being too far away from the laser points defining its object plane are eliminated. Finally, one of the remaining candidate points is chosen as result according to an intersection option selected by the user (i.e. the foremost or the hindmost point). In this way, the erroneous laser measurements close to edges and corners are avoided and furthermore, the distance from the image centre to the intersection point is determined with a better accuracy than the single laser point. This technique works best for images from mounted cameras, such as for the Riegl LMS Z420i, but can also be applied to other images.

The paper is structured in the following way: Section 2 gives an overview on related work. The detailed explanation of the proposed method is given in section 3, followed by two examples in section 4. An outlook in section 5 concludes the paper.

2. RELATED WORK

Our approach is closely related to mono-plotting in aerial photogrammetry, e.g. (Kraus 1996): From a single image the 3D coordinates of object points are determined by intersecting the respective projection rays with a given surface model; i.e. the points are 'plotted' on the surface. In recent years related work on applying mono-plotting to combined laser-image-data was published in different papers.

Perhaps one of the first approaches was the so-called '3D-orthophoto' (Forkert and Gaisecker 2002), later renamed to 'Z-coded true orthophoto' (ZOP) (Jansa et al. 2004). Here the image-laser-data is used to derive a true orthophoto with respect to a predefined object plane and with a certain ground resolution. The transition from this usual orthophoto to the ZOP is established by also computing the depth values of the orthophoto pixels with respect to the predefined object plane and adding this information as fourth layer to the three colour layers (red, green, blue).

Other authors apply the mono-plotting to the original images by mapping all laser points into the image and interpolating the object distance for all image pixels from these mapped points. Again, this distance information is stored as a fourth channel with the image. In (Bornaz and Dequal 2004) this resulting 4-dimensional image is termed 'solid image', and in (Abdelhafiz et al. 2005) this result is termed '3D image'.

The idea behind these 4-dimensional images and the ZOP is that the human operator just views the respective image, clicks on the points of interest and immediately gets the corresponding 3D coordinates. However, since here the original laser points are used for interpolating the distance of each image pixel either by nearest neighbour or by a simple average weighted method, the mentioned erroneous laser measurements close to edges and corners will to some extent remain in the results and may lead to unwanted smoothing effects.

The approach presented by (Becker et al. 2004) is closer to our method. Here also the original images and the associated laser data are used and only selected image points are determined in 3D space by intersecting image rays with 3D planes. The difference to our approach is that in (Becker et al. 2004) the operator first has to manually define the respective 3D plane in a view of the original image superimposed with the respective laser point cloud by selecting a certain area of supporting laser points. Afterwards the adjusting plane through that point set is determined, and from then on all further selected points in the original image will be mono-plotted with respect to this pre-defined plane. In our approach the respective object plane is determined automatically for each selected point, thus a higher degree of automation and a better adaptation to the shape of the object is achieved.

3. THE PROPOSED METHOD

Of the three phases mentioned in section 1 we only deal with the modeling phase in the context of this paper. Thus we assume the acquisition and orientation phase to be accomplished in advance. Therefore we know the camera's interior orientation, its relative orientation with respect to the scanner, and further the scanner's absolute orientation.

Consequently our problem is the following: Given the measured image co-ordinates of a point, we want to determine its 3D object coordinates using a raw, i.e. in no way pre-processed, laser scanner point cloud that covers the area of interest. With the known orientation, the image ray can be transformed to the co-ordinate system of the scanner.

Since the direction to the object point is already very precisely determined by the image ray, only the distance information is missing. The simplest approach would be to use the measured distance d_{meas} of the laser point P_{close} that is situated closest to the image ray and to intersect the image ray with the sphere with radius d_{meas} centred in the scanner's origin. This approach, however, has two drawbacks:

(i) It is not robust and thus not reliable: If P_{close} is near a depth discontinuity (i.e. close to an edge) the measured laser distance can be *systematically* wrong. A laser scan of an object of interest generally contains also points on non-interesting objects e.g. points on vegetation, on humans or cars passing by, etc. A scan may also contain blunders caused by failures of the measurement device. Consequently, if P_{close} is accidentally on one of these mentioned objects or a blunder, the selected distance will be *grossly* wrong.

(ii) It neglects possible accuracy improvements. Even if P_{close} is a valid laser measurement, its distance is still affected by random errors.

Both drawbacks can be eliminated if not only one point is considered but also its neighborhood. Consequently the task is to "intersect" the image ray with the point cloud. For this the following facts have to be considered:

- The laser point cloud is discrete. Therefore the covered region in the neighbourhood of the object point has to be approximated by a proper surface in order to compute the intersection with the image ray. The simplest approximation is by a plane, although in principle surfaces of higher order are also applicable.
- The laser measurements contain *random*, *systematic* and *gross errors*. In order to deal with the random errors the surface approximation has to be done using an adjustment and in order to deal with the systematic errors close to edges and gross errors in general this has to be done in a robust way.
- If the point of interest is situated on an edge or in a corner the respective image ray will in general intersect more than one object plane. Consider e.g. the planes of the oriel in fig. 1, where the image ray of a point on an oriel's edge will also intersect the plane of the façade of the house. The searched object point may be situated at the oriel's edge as well as in the façade's plane, since both possible 3D points are mapped to one and the same image point. In order to get a unique solution, the user has to specify which part of the object (the foremost or the hindmost) he or she is interested in.

The proposed method consists of two steps. In the first step, we extract the laser points from the point cloud that are situated within a certain neighbourhood of the image ray. More exactly, we define a "cone of interest". The axis of that cone coincides with the image ray, and its apex is the camera's projection centre. Its apex angle is chosen depending on the scan's angular step width. Only points inside this cone are considered for further analysis.

In the second step, the 3D co-ordinates of the point of interest are determined by intersecting the respective image ray with an object plane. For this at first, we set up plane hypotheses using an extension of the RANSAC (random sample consensus) framework (Fischler and Bolles 1981). Then, the intersection points between the image ray and the detected planes are calculated yielding candidates for the required object point. Candidates being too far away from the laser points defining its object plane are eliminated. Finally, one of the remaining candidate points is chosen as result according to an intersection option selected by the user (i.e. the foremost or the hindmost point).

3.1 Determination of the points inside the cone of interest

Solving this task is simplified by using the laser points' topological information, which is provided by most laser scanner systems. In case of the system Riegl LMS-Z420i, the measurements are arranged in a *measurement matrix*, where the column-row-index-space (c, r) and the direction-space (α, ζ) are related in the following way:

$$\alpha = \Delta_\alpha \cdot c + \alpha_0 \quad \text{and} \quad \zeta = \Delta_\zeta \cdot r + \zeta_0 \qquad (1)$$

where α is the horizontal direction, ζ the vertical direction, Δ_α the horizontal angle step width and Δ_ζ the vertical angle step width (usually $\Delta_\alpha = \Delta_\zeta = \Delta$), c the column index, r the row index, α_0 the horizontal direction at $c = 0$, and ζ_0 the vertical direction at $r = 0$.

Note that the directions α and ζ are only scheduled values. The actual direction measurement values (α_{meas}, ζ_{meas}) may slightly differ from the scheduled ones. These measurements (α_{meas}, ζ_{meas}) together with the measured distance and the intensity of the returned laser-pulse are stored in this matrix. Thus the measurement matrix actually contains 4 layers. Using only the intensity layer as grey value image, also called "intensity image" (cf. fig. 1b), the laser scanner data can be visualized in a simple way. Note, however, that only those cells in the data matrix are valid for which a distance measurement has been carried out successfully (cf. fig. 1b, where non-valid points appear blue).

In order to have enough points inside the cone of interest (which we denote by $\mathscr{C}$) we select a rather large apex angle of 20 times the angle step width Δ. For determining the points inside $\mathscr{C}$ we map $\mathscr{C}$ into the measurement matrix. Therefore, we have to project $\mathscr{C}$ first onto the unit sphere centred in the scanner's origin O, and afterwards transform it from the direction space to the column-row-index space using equations (1).

Apart from the cases where the image ray (which we denote by $\mathscr{R}$) contains the scanner's centre, its projection onto unit sphere is a part of a great circle (fig. 2a). Hence, this great circle arc is also the projection of the cone's axis. In order to get the whole spherical area of interest, we need the projection of the cone's contour (as seen from the scanner's centre O). The projections of the cone's contour generators are also great circle arcs. The set $\mathscr{G}$ of all generators' points at infinity corresponds to the intersection curve of the unit sphere with the parallel congruent cone $\mathscr{C}\|$ having its apex in the scanner's centre O. Hence, the image curve of $\mathscr{G}$ on the unit sphere is a small circle (fig. 2b).
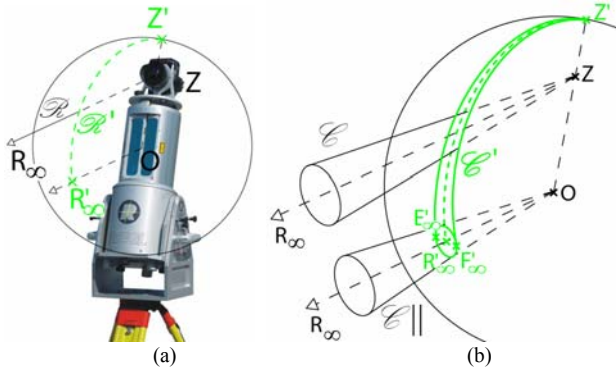

(a)   (b)

Fig. 2. (a): The laser scanner Riegl LMS-Z420i with mounted camera. An image ray $\mathscr{R}$ starting at the camera's projection centre Z is mapped onto unit sphere centered in the origin O of the scanner's co-ordinate system. The resulting image of the ray is a great circle arc between the image Z' of the projection centre and the vanishing point R_{∞}' of the ray's direction. (b): Cone of interest $\mathscr{C}$ around the ray $\mathscr{R}$ and its image on the unit sphere. E_{∞}' and F_{∞}' are the vanishing points of the cone's contour generators seen from the scanner's origin O.

Using the equations of the two great circle arcs through E_{∞}' and F_{∞}' in fig. 2b and the small circle, and by applying the transformation from direction space to column-row-index space, we can determine the window of interest in the measurement matrix. Afterwards, we check for each pixel within this window, if it has a valid distance and if the respective laser point is actually inside the cone of interest ("point-inside-cone test"). Fig. 3 shows an example for a measured image point and the projection of the respective cone of interest in the scan's intensity image.

As result of this first step, we obtain a set of points near the image ray (represented by the green pixels in fig. 3b), which is the basis for further analyses.

3.2 Detection of object planes and determination of the 3D co-ordinates of the point of interest

In order to determine the 3D co-ordinates of the point of interest, we have to estimate a laser distance for the digitised image point using the obtained set of points inside the cone of interest. It was already argued in the beginning of section 3 that a reliable determination of such a distance by intersection with the respective image ray requires a surface approximation in the vicinity of the point of interest. The simplest approximation is by a plane, although in principle surfaces of higher order are also applicable.

We assume that up to i_{max} (e.g. $i_{max} = 5$) planes are to be found in the vicinity of the point of interest (i.e. in the cone of interest). Our approach for detecting them is based on the RANSAC framework. At the beginning, all points are unclassified, i.e. none of them is assigned to any plane. Plane detection is done iteratively. In each step ($i = 1, \dots i_{max}$), that plane π_i is detected which has the highest support from the unclassified points. The supporting points are then classified as belonging to the detected plane.
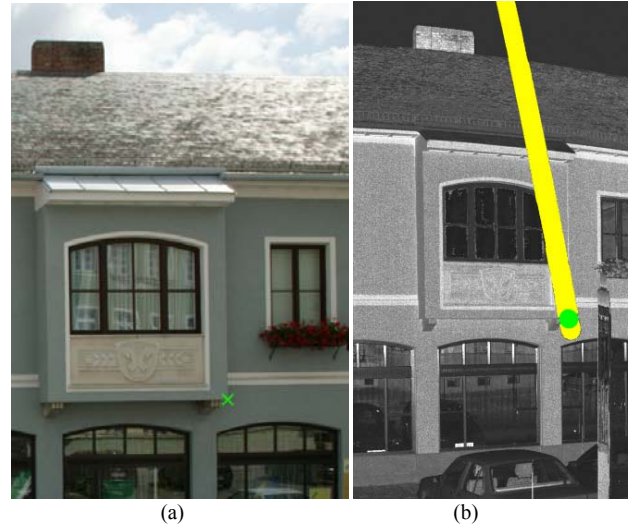

(a)   (b)

Fig. 3. (a): Section of a photo with measured image point (green cross). (b): Section of the scan's intensity image. The pixels inside the spherical image of the respective cone of interest are marked in yellow; those also fulfilling the point-inside-cone test are marked in green.

Although in each step only one plane (the one with largest support) is detected, for finding this plane several plane hypotheses γ_k ($k = 1, \dots k_{max}$) are tested based on an adapted RANSAC approach. Finding planes using RANSAC in its original form would mean that we would have to randomly select the minimum number of three points and test the remaining points for incidence with this plane. However, we only select one seed point for each plane hypothesis. Then, we select all neighbouring points within a sphere of radius ε_1, which is chosen dependent both on the angular step width Δ of the laser scan and the laser distance measured at the seed point d_S as $\varepsilon_1 = 3 d_S \Delta$. Thus, 20-30 points will be selected. A plane

hypothesis γ_k is generated by calculating a least-squares plane through the seed point and the selected neighbours. This plane can also be considered as a tangential approximation to the laser points in the seed point. Summarizing, our modified RANSAC method differs from the classical one by the following:

- Each of the n points inside the cone of interest could be used to create a plane hypothesis. Thus, the maximum number of possible hypotheses is n compared with "n choose 3" in classical RANSAC. k_{max}, the number of hypotheses that have to be checked in order to find at least one seed point in one of the up to i_{max} possible planes with a probability of 99.9% is given by $\ln(0.001)/\ln(1-1/i_{max}) \sim 31$.
- The plane hypotheses are set up locally by least-squares adjustment compared to a direct solution through 3 points at classical RANSAC.
- This modified approach tends to suppress the generation of hypotheses merging two or more slightly different planes to a single one and therefore obtaining unjustifiably high support. In other words, our modified method provides more robustness against unjustified merging of planes.

A point supports a plane hypothesis if its orthogonal distance to the plane is within $\pm\varepsilon_2$, which is the standard deviation (in direction of the plane-normal) derived from the seed point's co-variance matrix. The latter is derived from the accuracies of the laser scanner. Of all the plane hypotheses γ_k the plane π_i having the highest support, i.e. the plane explaining most unclassified data points, is accepted. Afterwards, π_i is re-adjusted using all its supporting points.

The points in this supporting set, however, are not yet finally assigned to π_i. The assignment of an unclassified data point to the plane π_i is based on a statistical test (significance level e.g. 5%). This test considers the points' orthogonal distance to π_i and the covariance matrices of π_i and of the points (derived from the laser scanner accuracies). This is favoured over a simple (non-statistical) distance threshold criterion, because the accuracy of a laser point in Cartesian space may be rather anisotropic. Especially in case of short distances (< 10m), a point is significantly better determined perpendicularly to the laser beam than in radial direction. In other words, the noise perpendicular to the plane heavily depends on the angle between plane normal and laser beam.

For the remaining unclassified points the next plane with maximum support π_{i+1} is detected, and so on. The process will stop after the maximum number of "best" planes π_i ($i_{max} = 5$) has been detected or if only a small percentage (e.g. 10%) of points is still unclassified. As result, we get a set of planes together with their associated data points.

Each plane π_i is intersected with the image ray yielding candidates S_i for the desired intersection point. However, we can immediately reject those candidate-points that are situated far away from any data point assigned to the respective plane π_i. Therefore, for each candidate point S_i, we determine the closest data point P_i belonging to its underlying plane, and calculate the distance between S_i and P_i. A candidate point is rejected if this distance exceeds a distance ε_3, which depends on the distance d_S of S_i to the scanner's origin and the scan's angular step width Δ as $\varepsilon_3 = 2d_S\Delta$.

Finally, one of the remaining candidate-points is accepted according to the selected user option, which may be intersection with either the foremost or the hindmost plane. In this way we obtain the 3D co-ordinates of the object point measured in the photo in the beginning. If there are additional observations to the same point (e.g. in other photos), its calculated laser distance together with its image co-ordinates may be introduced as observations in a subsequent adjustment.

4. EXAMPLES

In this section, we give two typical examples in order to demonstrate our approach. In case of the first example, three planes were detected (fig. 4). Depending on the user option, either plane 2 or plane 1 is intersected with the ray. In this case plane 2 is used (i.e. the foremost plane) since the user is interested in the oriel's corner. Note that our approach delivers a reasonable result, although the image ray runs through an area of erroneous laser points near distance discontinuities.

Fig. 5 shows another example, where the maximum number of planes ($N_{max} = 5$) was detected. Compared with the previous example, the proportion of erroneous points is relatively small. However, this is a good example in order to argue why we do not use the original RANSAC approach (generation of hypothesis by 3 random points) for plane detection: Due to the poor extension/noise ratio of plane 3, the original RANSAC approach tends to merge the points of plane 3 with some of those situated on the (parallel) front plane of the oriel's corbel, which is about 5cm behind. Hence, the hypothesis having the highest support would deliver a tilted plane – and therefore a wrong intersection point. However, our adapted RANSAC approach is able to separate those two different planes, since it is more robust against merging of noisy similar planes. The desired point (the oriel's corner) is obtained by intersecting the image ray either with plane 1 or plane 3. Note that the distance between the respective intersection points is only 5mm (compared with the distance measurement accuracy of ± 1cm). Thus the error of choosing a wrong neighbouring plane is smaller than the original measurement accuracy. However, as this example shows a further improvement of the proposed method could be achieved by determining the object point of interest not only by intersecting the image ray with one plane but to include (if present in the laser data) up to two intersecting planes in case the point lies on an edge or up to three planes in case the point is a corner. Fig. 5 also shows an unwanted property of the current implementation of the RANSAC approach, that due to the "first come first serve" classification points, which would better fit to plane 4 are classified to the more dominant plane 1. Same holds for the planes 3 and 2. We will adapt this by region-based analyses in the next implementation.

Anyway, the two examples show that our approach is able to deal with blunders, systematic errors and measurement noise.
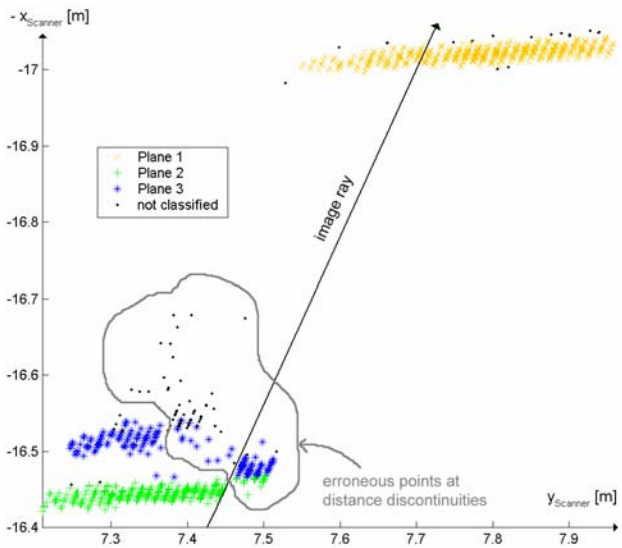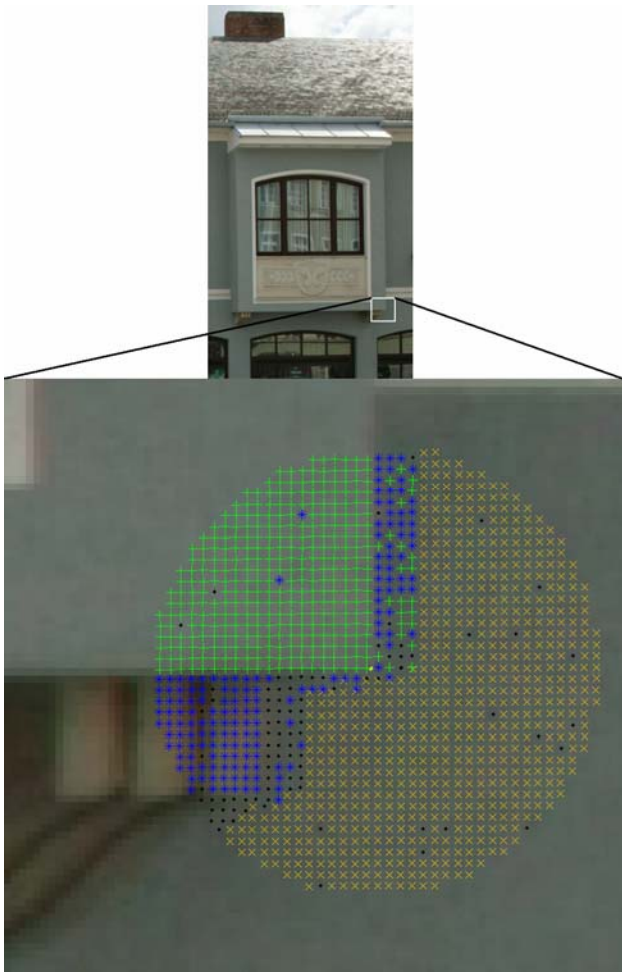
Fig. 4. Laser points near image ray after classification (cf. fig. 3). Top: Projection into photo. Bottom: Ground view.
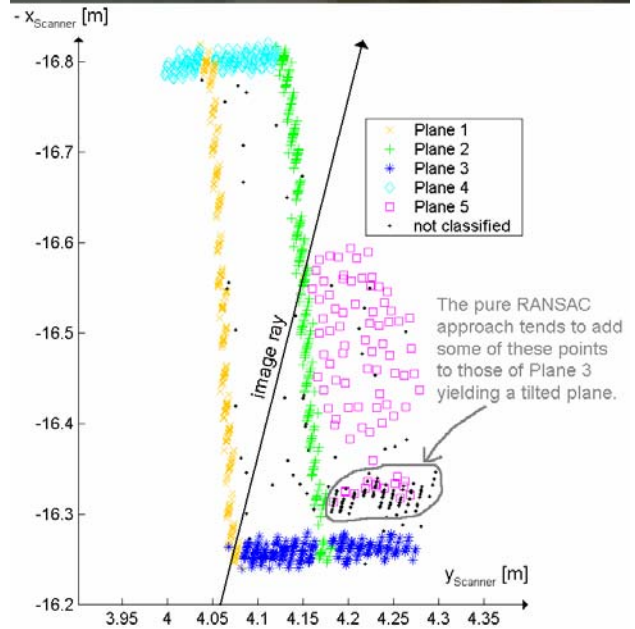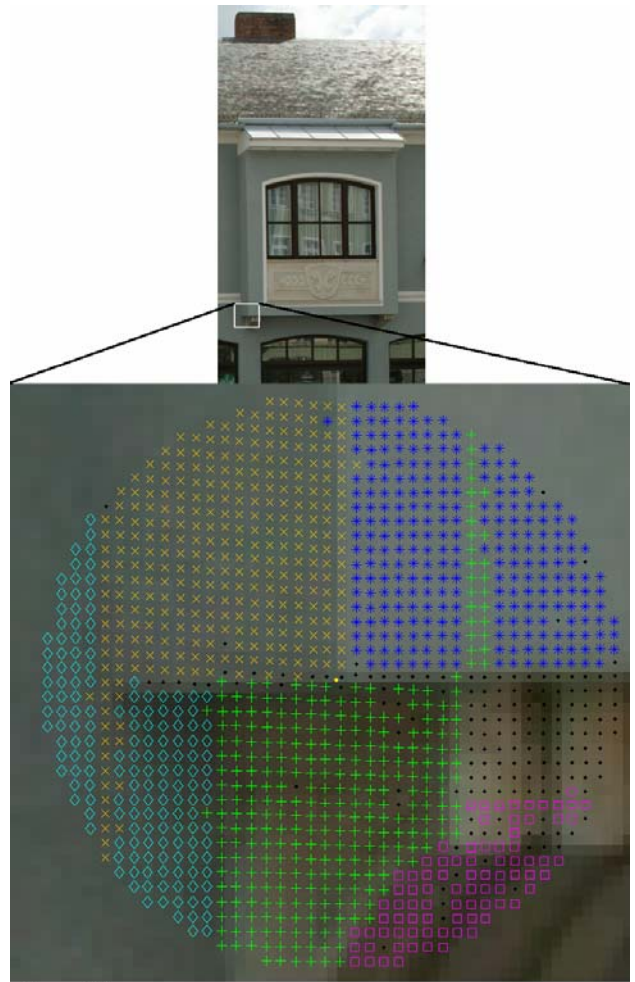

Fig. 5. Another example after classification of the laser points. Top: Projection into photo. Bottom: Ground view.

5. SUMMARY AND OUTLOOK

We presented a concept for mono-plotting using combined image and laser data. The idea is that a human operator first selects the relevant modelling points manually in the high resolution images, thereby performing the necessary generalization. Then the 3D coordinates of the respective object points are obtained by intersecting the image ray with a surface patch. The latter is extracted by analyzing the laser points in a cone of interest around the image ray. We search for planes with the highest support from the laser points, which is motivated by considering primarily objects that can be represented by polyhedral compounds. Surface patches of higher order, however, could also be applied for other applications.

The main properties of this approach are: (i) it is *adaptive*, in the sense that for each selected image point a well suited plane from the laser data is searched for, (ii) gross and systematic *errors in the laser data are removed* and due to the adjusting surface patch the distance to the object points is derived with a better accuracy than the single laser point measurement.

Future work should be directed in two ways:
(i) Increase the automation of surface modelling using combined image and laser data. From a geometric point of view the redundancy in the image and laser data, especially concerning edges, which can be extracted automatically to a high degree in both data sets, is promising. From a semantic point of view this task, however, is rather challenging, as the rate and method of generalization is difficult to automate and will involve many aspects from artificial intelligence. Therefore this task will remain relevant within the respective communities (photogrammetry, computer vision, cartography …) for the coming years, perhaps even decades.

(ii) In the meantime the proposed mono-plotting method is a promising tool to speed up object modelling. Therefore it is worth investigating the amount of time that can be saved using our method, e.g. by comparing the time required to model a certain large object by this mono-plotting method and by other methods. Also the accuracy achieved by the proposed method needs to be analyzed, although the term *accuracy* in the context of surface modelling also involves aspects of generalization. Further the method for deriving the (planar) patch of highest support from the laser data may have room for improvement (cf. sec. 4). An alternative to the already implemented RANSAC approach would be a Hough-transform-like approach (e.g. (Pottmann et al. 2002)), where for each laser point in the cone of interest its tangential plane is estimated using the neighbouring points. Afterwards in the parameter-room of these planes the clusters of planes are analyzed. We will work on theses issues in the future.

6. ACKNOWLEDGEMENT

7. REFERENCES

Abdelhafiz A., Riedel B., Niemeier W., 2005. "3D Image" As A Result From The Combination Between The Laser Scanner Point Cloud And The Digital Photogrammetry, *Optical 3-D Measurement Techniques VII*, (Eds. A. Grün and H. Kahmen), Volume 1: 204-213

Becker R., Benning W., Effkemann, C., 2004. Kombinierte Auswertung von Laserscannerdaten und photogrammetrischen Aufnahmen, *Zeitschrift für Vermessungswesen*, Heft 5: 347-355

Böhler W., Bordas Vicent M., Marbs A., 2003. Investigating Laser Scanner Accuracy, *The International Archives of* Photogrammetry*, Remote Sensing and Spatial Information Sciences*, Antalya , Vol. XXXIV, Part 5/C15: 696-701

Bornaz L., Dequal S., 2003. The Solid Image: An Easy And Complete Way To Describe 3D Objects, *The International Archives of* Photogrammetry*, Remote Sensing and Spatial Information Sciences*, Antalya , Vol. XXXIV, Part 5/C15.

Fischler M. A., Bolles R. C. Random Sample Consensus, 1981: A Paradigm for Model Fitting with Applications to Image Analysis and Automated Cartography. *Comm. of the ACM*, Vol 24, pp 381-395.

Forkert G., Gaisecker Th., 2002. *3D Rekonstruktion von Kultur-gütern mit Laserscanning und Photogrammetrie*, Oral presentation at the CULTH2 congress "Die Zukunft des Digitalen Kulturellen Erbes" at the MUMOK, Vienna, Jan. 13 – 14 2002.

Jansa J., Studnicka N., Forkert G., Haring A., Kager H., 2004. Terrestrial Laserscanning and Photogrammetry - Acquisition Techniques Complementing One Another; in: O. Altan (Ed.); *Proceedings of the ISPRS* XXth Congress, Vol XXXV, Part B/7, Istanbul, July 12 – 23 2004; ISSN 1682-1750; 948 - 953.

Kraus K, 1996. *Photogrammetry*, Volume 2: Advanced Methods and Applications, Third edition, Dümmler/Bonn.

Pottmann H., Leopoldseder S., Wallner J., Peternell M., 2002. Recognition and reconstruction of special surfaces from point clouds. *International Archives of Photogrammetry and Remote Sensing*, Graz, Austria, Vol. XXXIV, Part 3A, pp. 271-276.

Riegl, 2006. http://www.riegl.co.at/ [Accessed: 2006-03-24]

Rottensteiner F., 2001. Semi-automatic extraction of buildings based on hybrid adjustment using 3D surface models and management of building data in a TIS, PhD Thesis, Institute of Photogrammetry and Remote Sensing, Vienna, 189 pages